

Journal: Biomaterials Science  
Article type: Communication

## Supplementary Information

Title: Hierarchically structured hydrogels utilizing multifunctional assembling peptides for 3D cell culture

*Amber M. Hilderbrand<sup>1</sup>, Eden M. Ford<sup>1</sup>, Chen Guo<sup>1</sup>, Jennifer D. Sloppy<sup>2</sup>, April M. Kloxin<sup>1,2\*</sup>*

<sup>1</sup>Department of Chemical and Biomolecular Engineering  
University of Delaware  
150 Academy Street, Newark, DE 19716, USA

<sup>2</sup>Department of Material Science and Engineering  
University of Delaware  
201 DuPont Hall, Newark, DE, 19716, USA

\*Correspondence and requests for materials should be addressed to A.M.K. (email: [akloxin@udel.edu](mailto:akloxin@udel.edu))

## Table of Contents

Supplemental Figures.....	3
<b>Figure S1:</b> Single Quadrupole Detector 2 (SQD2) UPLC trace and ESI+ mass spectrometry of mfCMP-1a .....	3
<b>Figure S2:</b> Single Quadrupole Detector 2 (SQD2) UPLC trace and ESI+ mass spectrometry of mfCMP-2a .....	4
<b>Figure S3:</b> Wavelength scans of a) mfCMP-1a and b) mfCMP-2a .....	5
<b>Figure S4:</b> TEM of mfCMP-2a assembled at 0.3 mM.....	6
<b>Figure S5:</b> mfCMP-1 assembling control peptide without alloc .....	7
<b>Figure S6:</b> <i>In situ</i> oscillatory rheology of hydrogels that contain 2.5 mM mfCMP- 2a .....	8
<b>Figure S7:</b> Circular dichroism data on hydrogels with and without 2.5mM mfCMP-1a .....	9
<b>Figure S8:</b> Object shape factor histograms for cells in 3D cultures .....	10
<b>Figure S9:</b> Cell viability and morphology in hydrogels with mfCMP-2a .....	11
<b>Table S1:</b> Viability of hMSCs cultured in hydrogels with 0 mM, 1 mM, or 2.5 mM of mfCMP-1a.....	12
<b>Table S2:</b> Results of statistical analysis of CMP-1a viability using a Student's T-test.....	12
<b>Table S3:</b> Shape factor analysis of hMSCs in hydrogels containing 0 mM, 1 mM, or 2.5 mM mfCMP-1a.....	12
<b>Table S4:</b> Statistical analysis of shape factor distribution of cells cultured in hydrogels containing mfCMP-1a using a Student's test.....	12
Supplemental Figures to Support Methods.....	13
<b>Figure S10:</b> ESI+ spectrum for mfCMP-1 (PKG) <sub>4</sub> (POG) <sub>6</sub> (DOG) <sub>4</sub> .....	13
<b>Figure S11:</b> Scheme of Fmoc-GPO(tBu)-OH fragment synthesis.....	14
<b>Figure S12:</b> <sup>1</sup> HNMR spectrum of Fmoc-Gly-OSu fragment .....	15
<b>Figure S13:</b> <sup>1</sup> HNMR spectrum of Fmoc-GP-OH .....	16
<b>Figure S14:</b> <sup>1</sup> HNMR spectrum of Fmoc-GP-OSu .....	17
<b>Figure S15:</b> <sup>1</sup> HNMR spectrum of Fmoc-GPO(tBu)-OH .....	18
<b>Figure S16:</b> UPLC trace and ESI+ spectrum for linker peptide KK(aloc)GGPQGIWGQGK(aloc)K.....	19
<b>Figure S17:</b> UPLC trace and ESI+ spectrum for integrin binding peptide K(aloc)GWGRGDS .....	20
<b>Figure S18:</b> <sup>1</sup> HNMR spectrum of PEG-4-SH .....	21
<b>Figure S19:</b> <sup>1</sup> HNMR spectrum of LAP photoinitiator .....	22
<b>Figure S20:</b> Day 10 image splits of cells cultured within hydrogels with mfCMP-1a .....	23
<b>Figure S21:</b> Day 10 image splits of cells cultured within hydrogels with mfCMP-2a .....	24
<b>Figure S22:</b> Velocity processing for shape factor analysis.....	25
<b>Figure S23:</b> Velocity shape factor analysis and binning examples .....	26

## SUPPLEMENTAL FIGURES

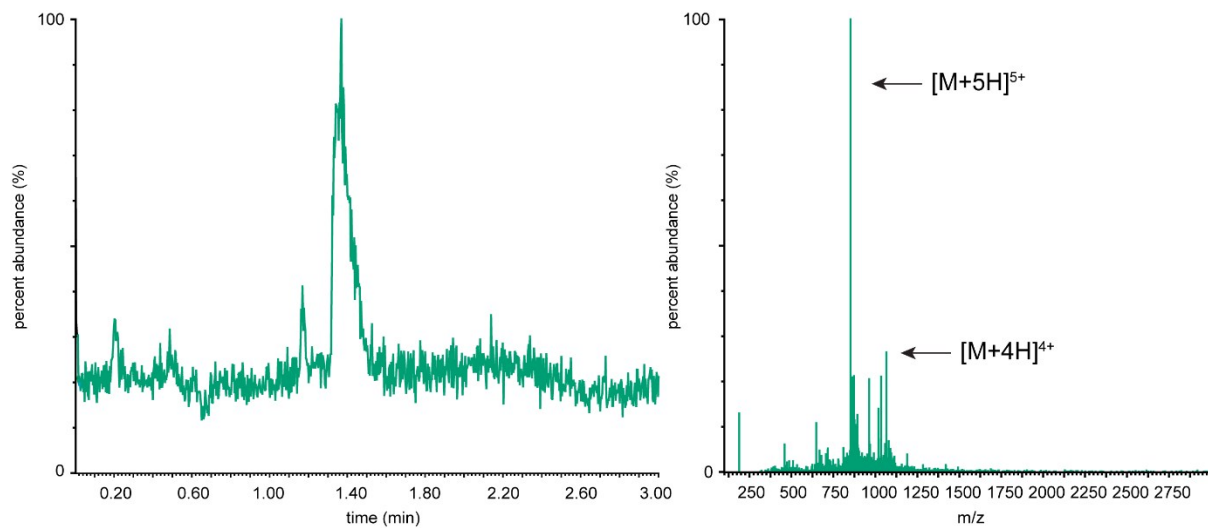


**Figure S1:** Single Quadrupole Detector 2 (SQD2) UPLC trace and ESI+ mass spectrometry of mfCMP-1a. The desired product was observed with expected molecular weight of 4256 g/mol ( $[M+4H]^{4+}$  = 1065 g/mol and  $[M+5H]^{5+}$  = 852 g/mol).

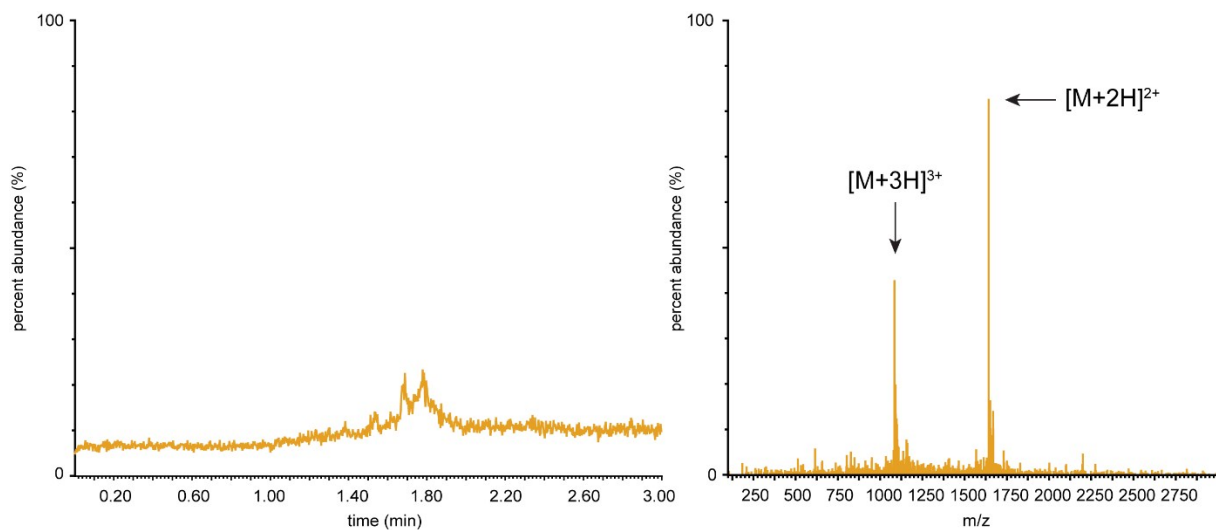


**Figure S2:** Single Quadrupole Detector 2 (SQD2) UPLC trace and ESI+ mass spectrometry of mfCMP-2a. The desired product was observed with expected molecular weight of 3287 g/mol ( $[M+2H]^{2+}$  = 1644 g/mol and  $[M+3H]^{3+}$  = 1096 g/mol).

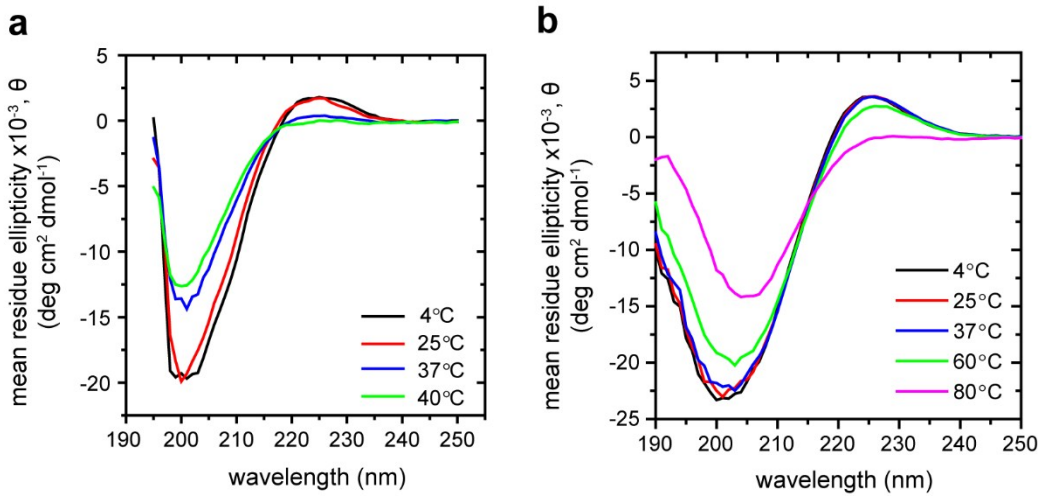


**Figure S3:** Wavelength scans of **a**) mfCMP-1a (0.1 mM in DPBS) and **b**) mfCMP-2a (0.1 mM in deionized water). Characteristic peak for triple helix at 225 nm was observed in both cases.

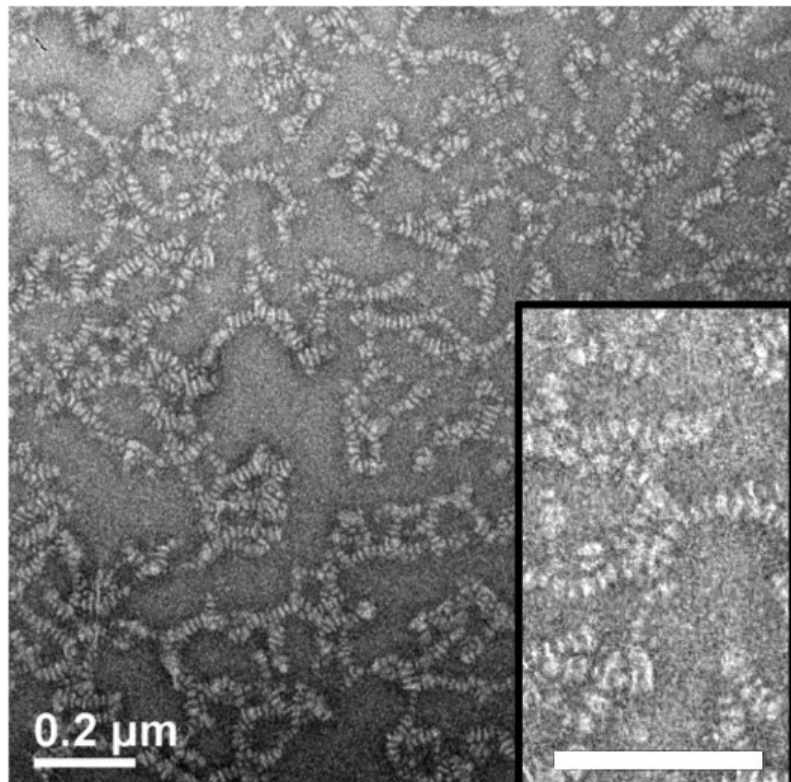


**Figure S4:** TEM of mfCMP-2a assembled at 0.3 mM (~1 mg/mL). Zoom in shows a striped morphology reminiscent of D-periodic banding structure found in native collagen. Scale bars = 0.2  $\mu$ m.

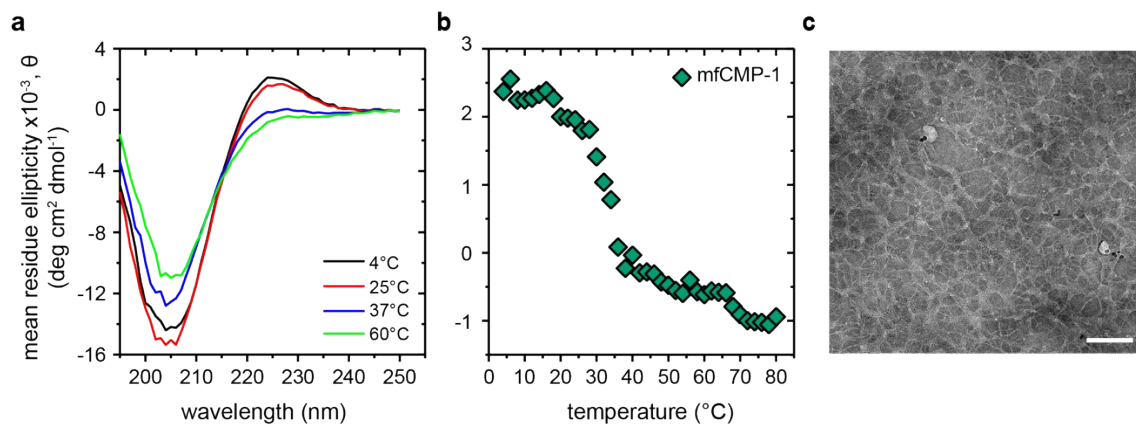


**Figure S5:** mfCMP-1 assembling control peptide without alloc. **a)** CD wavelength scans for mfCMP-1 in sodium phosphate demonstrated triple helix formation in solution. **b)** Mean residue ellipticity at 225 nm measured over a range of temperatures, where  $T_m$  of  $\sim 36$  °C was observed. **c)** TEM of mfCMP-1 assembled at 0.3 mM in 10 mM sodium phosphate demonstrated the formation of fibrils similar to those observed with mfCMP-1a. Scale bar = 200 nm.

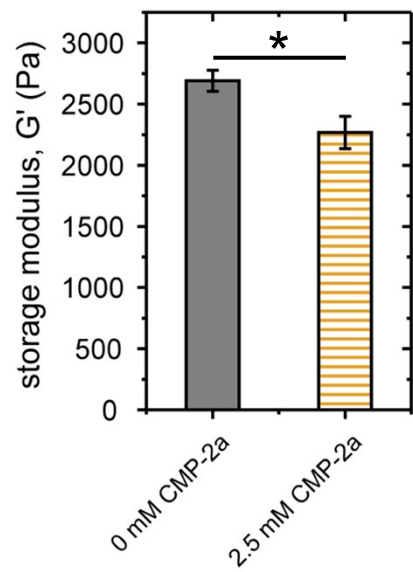


**Figure S6:** *In situ* oscillatory rheology of hydrogels that contain 2.5 mM mfCMP- 2a. A slight statistical difference in storage modulus was observed when compared to the control (n = 4; \*p < 0.05).

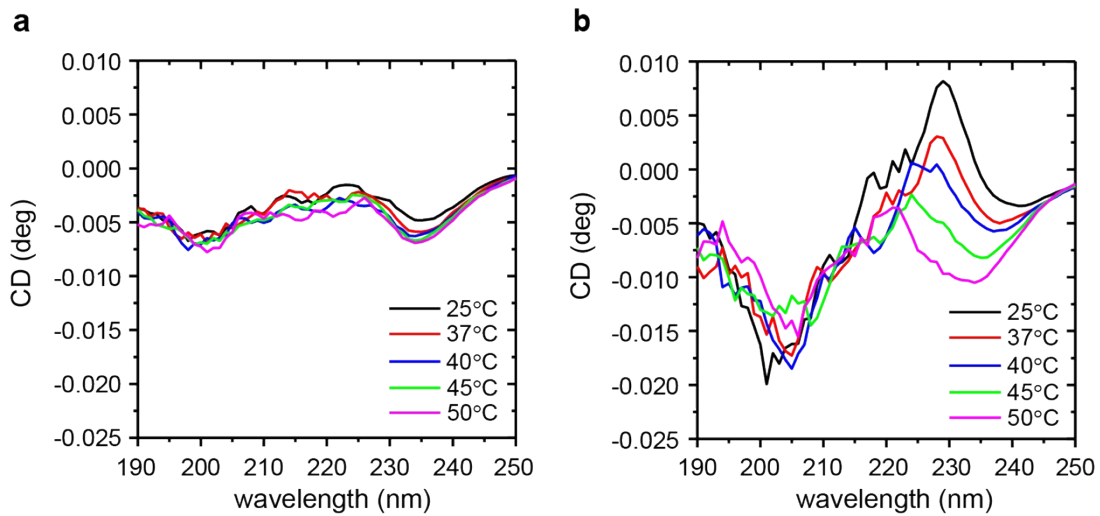


**Figure S7:** Circular dichroism data on hydrogels with and without 2.5mM mfCMP-1a. **a)** Wavelength scans of 6 wt% PEG-SH hydrogels that contain 0 mM mfCMP-1a at various temperatures. **b)** Wavelength scans of 6 wt% PEG-SH hydrogels that contain 2.5 mM mfCMP-1a, where peak at  $\sim 231$  nm is indicative of a triple helix and decreases with increasing temperature as the triple helices are melted.

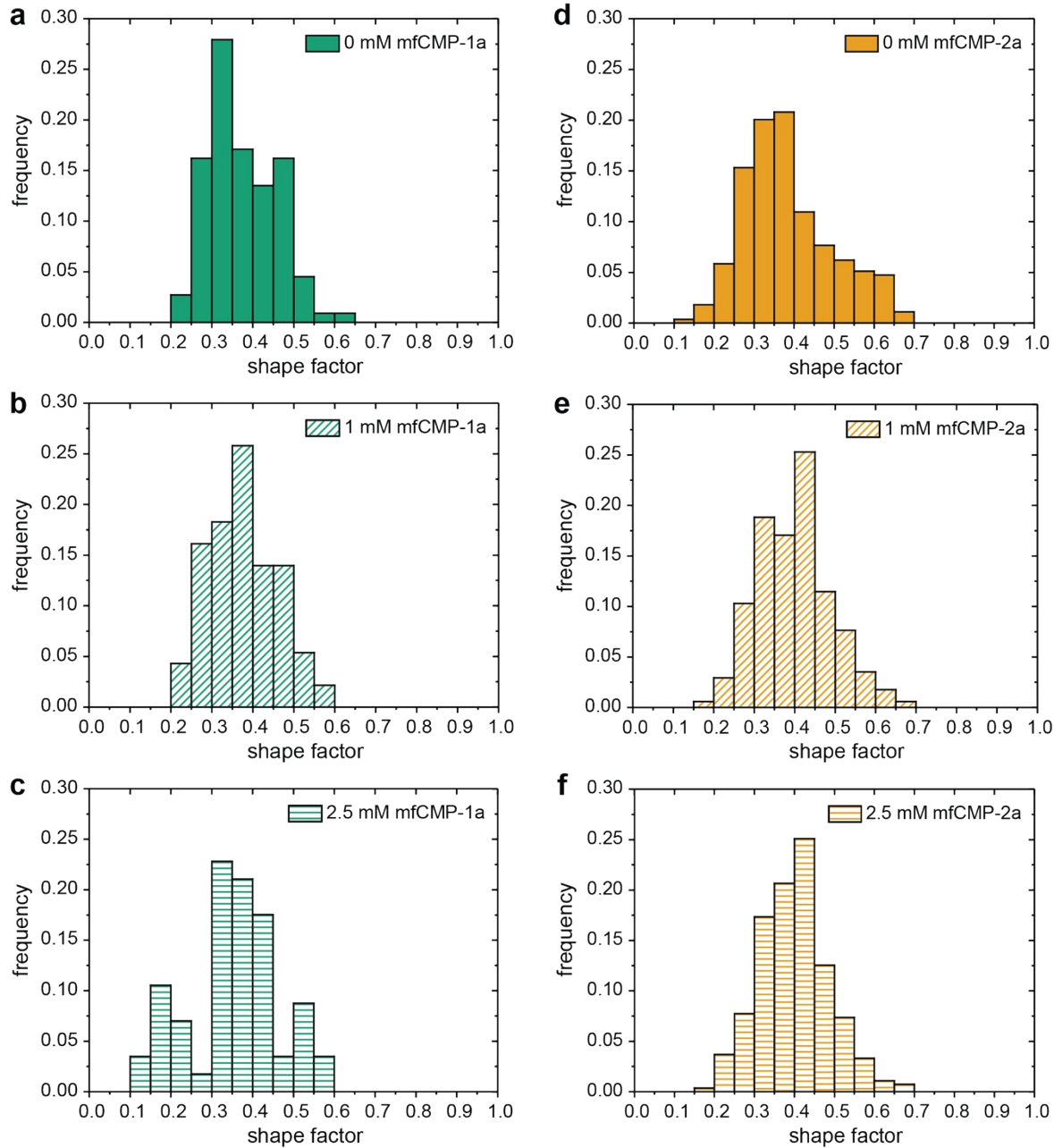


**Figure S8:** Object shape factor histograms for cells in 3D cultures. Cell morphology was analyzed through quantification of 3D shape factor ( $\Psi$ ) of objects (individual or clusters of cells) at day 10 for hydrogels containing **a**) 0 mM mfCMP-1a, **b**) 1 mM mfCMP-1a, or **c**) 2.5 mM mfCMP-1a and **d**) 0 mM mfCMP-2a, **e**) 1 mM mfCMP-2a, or **f**) 2.5 mM mfCMP-2a. Shape factor distributions were used to set bins for *elongated* ( $0 \leq \Psi \leq 0.25$ ), *spread* ( $0.25 < \Psi \leq 0.5$ ), and *rounded* ( $0.5 < \Psi \leq 1$ ) objects based on the emergence of multiple modes in conditions with higher mfCMP concentrations, especially in mfCMP-1a ( $n = 3$  hydrogels,  $> 50$  objects or 100 cells counted per condition).

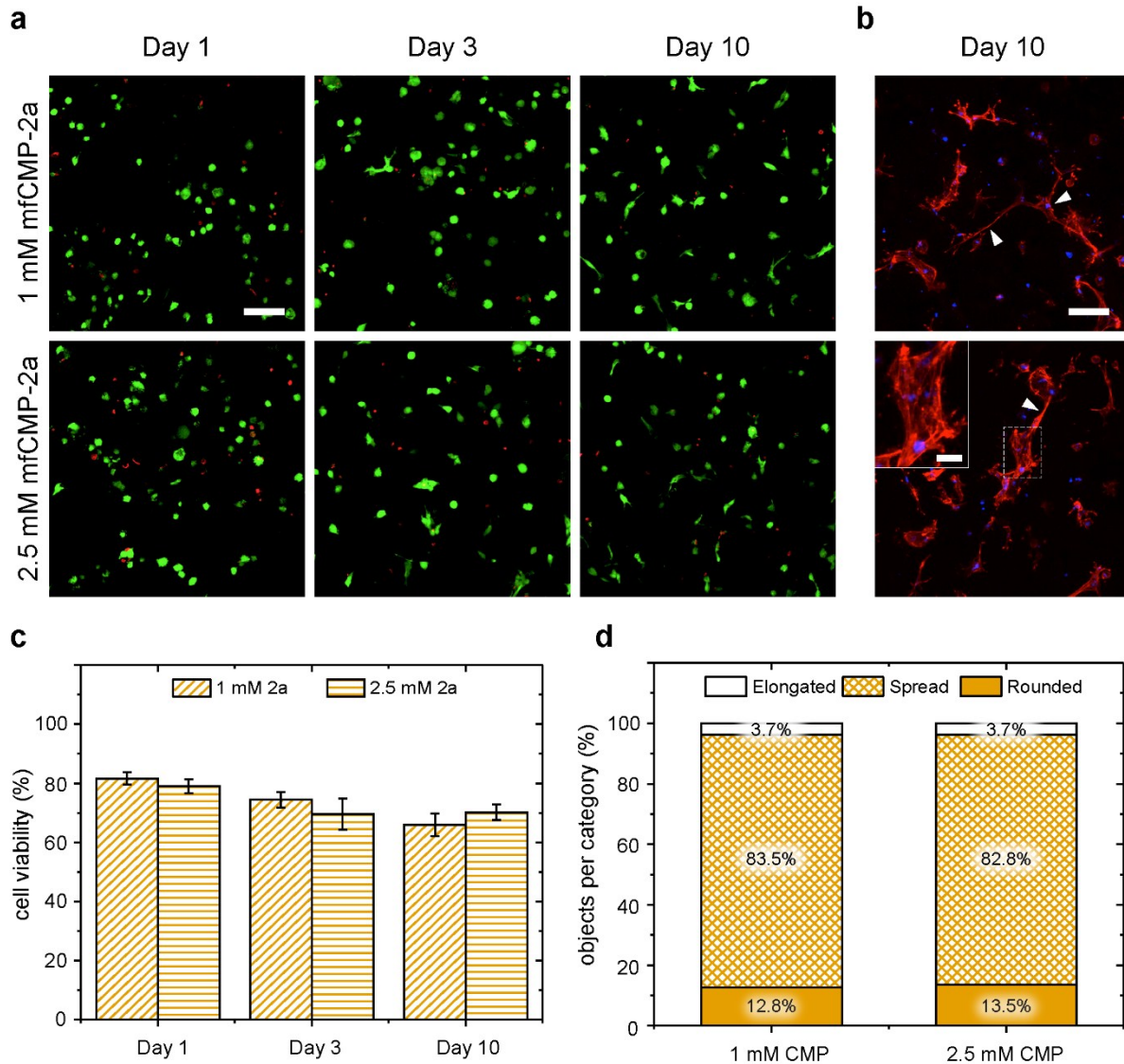


**Figure S9:** Cell viability and morphology in hydrogels with mfCMP-2a. Representative maximum intensity projections (from z-stacks, 200  $\mu\text{m}$  thick) of hMSCs encapsulated within hydrogels at a low concentration (1 mM) or at a high concentration (2.5 mM) of mfCMP-2a: **a**) cells stained for viability on days 1, 3, and 10, where live cells are shown in green and dead cell nuclei in red and **b**) fixed cells stained for F-actin in red and cell nuclei in blue on day 10 (Scale bars: full image = 100  $\mu\text{m}$ , inset image = 25  $\mu\text{m}$ ; arrowheads note long ‘chains’ of interacting hMSCs). **c**) Cell viability was quantified at days 1, 3, and 10 for hydrogels containing 1 and 2.5 mM mfCMP-2a (error bars represent the standard error around the mean;  $n = 3$  hydrogels,  $> 700$  cells counted per condition;  $*p < 0.05$ ,  $**p < 0.005$ ,  $***p < 0.0005$ ). **d**) Cell morphology was analyzed through quantification of 3D shape factor ( $\Psi$ ) of objects (individual or groups of cells) at day 10 for hydrogels containing 1 and 2.5 mM mfCMP-2a. Results for each hydrogel composition are shown as the percent of *elongated*, *spread*, or *rounded* objects (cells or cell clusters) within the sampled population ( $n = 3$  hydrogels,  $> 250$  objects or 400 cells counted per condition; no statistical differences observed).

**Table S1:** Viability of hMSCs cultured in hydrogels with 0 mM, 1 mM, or 2.5 mM of mfCMP-1a.

	0 mM CMP		1 mM CMP		2.5 mM CMP	
	Average	Standard Error	Average	Standard Error	Average	Standard Error
Day 1	93%	2.9%	91%	2.1%	84%	4.1%
Day 3	88%	3.0%	86%	1.9%	85%	4.4%
Day 10	85%	3.0%	87%	2.2%	88%	3.8%

**Table S2:** Results of statistical analysis of CMP-1a viability using a Student's T-test.

	0 mM CMP vs. 1 mM CMP	0 mM CMP vs. 2.5 mM CMP	1 mM CMP vs. 2.5 mM CMP
Day 1	0.291	0.005 **	0.017 *
Day 3	0.338	0.245	0.551
Day 10	0.386	0.298	0.676

\*p < 0.05

\*\*p < 0.01

**Table S3:** Shape factor analysis of hMSCs in hydrogels containing 0 mM, 1 mM, or 2.5 mM mfCMP-1a.

	0 mM CMP		1 mM CMP		2.5 mM CMP	
	Average	Standard Error	Average	Standard Error	Average	Standard Error
Rounded	8.0%	4.8%	6.6%	3.5%	13%	1.5%
Spread	89%	5.1%	89%	5.4%	59%	8.3%
Elongated	2.8%	1.4%	4.0%	2.0%	28%	7.7%

**Table S4:** Statistical analysis of shape factor distribution of cells cultured in hydrogels containing mfCMP-1a using a Student's T-test.

	0 mM CMP vs. 1 mM CMP	0 mM CMP vs. 2.5 mM CMP	1 mM CMP vs. 2.5 mM CMP
Rounded	0.825	0.420	0.191
Spread	0.971	0.038 *	0.039 *
Elongated	0.669	0.032 *	0.039 *

\*p < 0.05

## SUPPLEMENTAL FIGURES TO SUPPORT METHODS

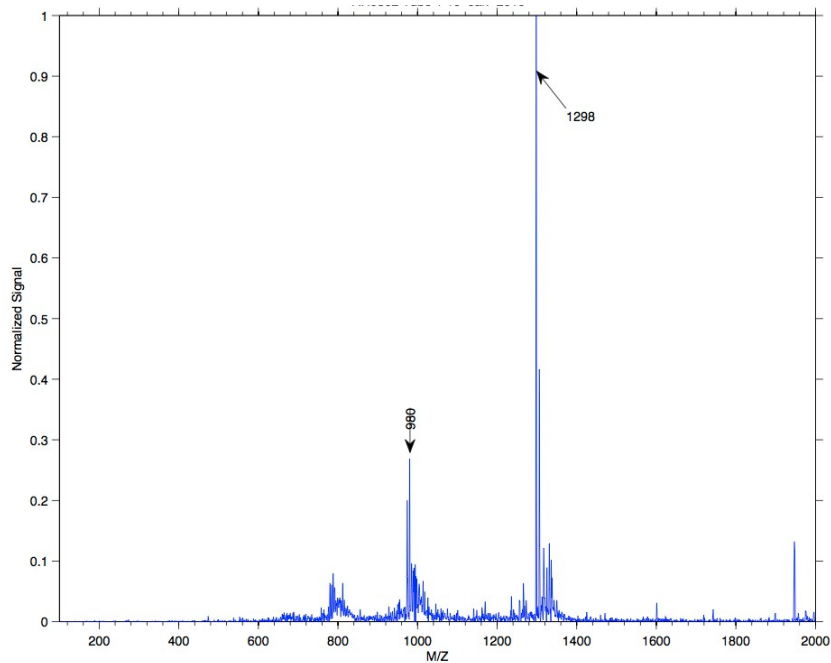


**Figure S10:** ESI<sup>+</sup> spectrum for mfCMP-1 (PKG)<sub>4</sub>(POG)<sub>6</sub>(DOG)<sub>4</sub>. ESI<sup>+</sup> mass spectrometry confirms the desired product with expected molecular weight of 3891 g/mol ( $[M+3H]^{3+} = 1298$  g/mol and  $[M+3H+Na]^{4+} = 980$  g/mol).

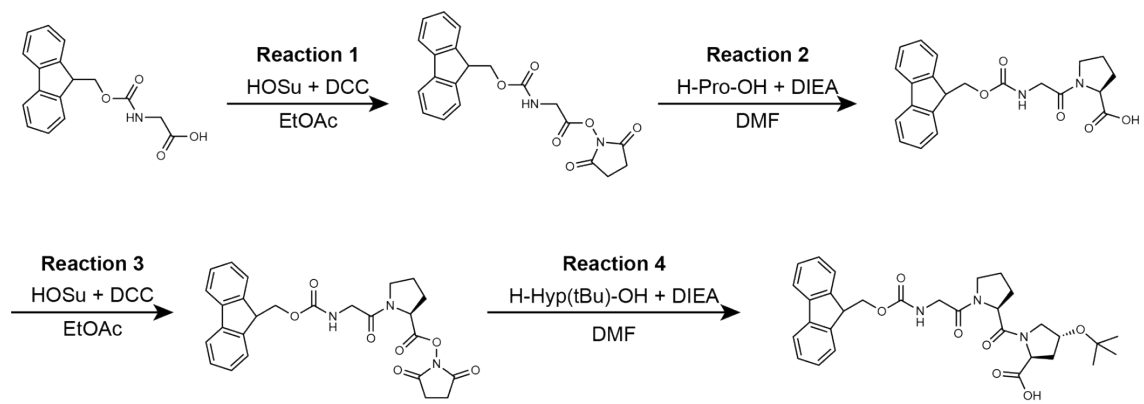


**Figure S11:** Scheme of Fmoc-GPO(tBu)-OH fragment synthesis.

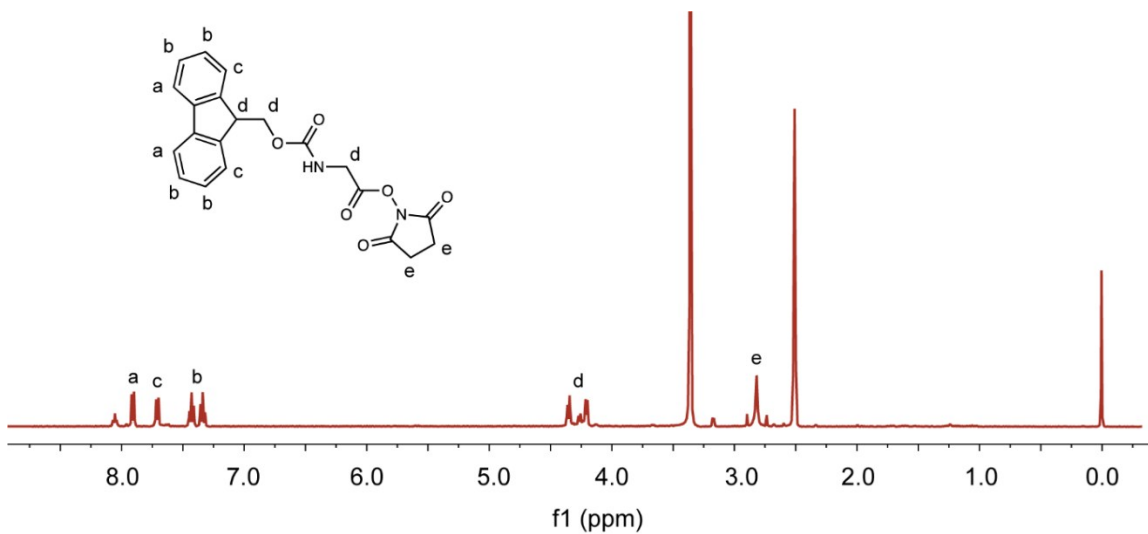


**Figure S12:**  $^1\text{H}$ NMR spectrum of Fmoc-Gly-OSu fragment.  $^1\text{H}$  NMR (400 MHz,  $\text{DMSO}-d_6$ )  $\delta$  7.91 (d,  $J = 7.5$  Hz, 2H), 7.71 (d,  $J = 7.4$  Hz, 2H), 7.47 – 7.29 (m, 4H), 4.40 – 4.17 (m, 5H), 2.91 – 2.72 (m, 4H).

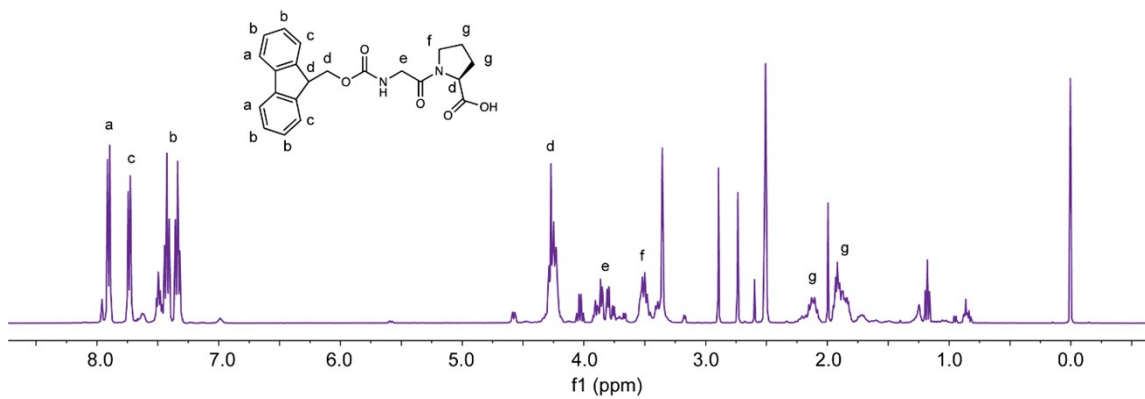


**Figure S13:** <sup>1</sup>H NMR spectrum of Fmoc-GP-OH. <sup>1</sup>H NMR (400 MHz, DMSO-*d*<sub>6</sub>) δ 7.90 (d, *J* = 7.5 Hz, 2H), 7.73 (d, *J* = 7.5 Hz, 2H), 7.46 – 7.29 (m, 4H), 4.37 – 4.16 (m, 4H), 3.94 – 3.73 (m, 2H), 3.51 (qd, *J* = 9.9, 8.2, 2.9 Hz, 2H), 2.17 – 2.04 (m, 1H), 1.96 – 1.77 (m, 3H).

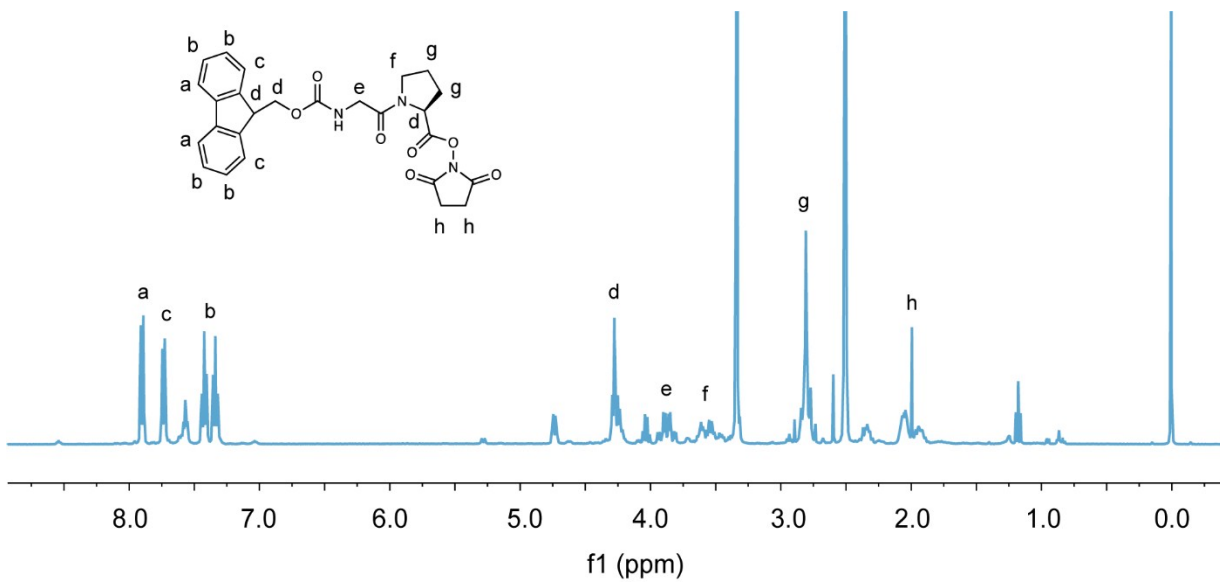


**Figure S14:**  $^1\text{H}$ NMR spectrum of Fmoc-GP-OSu.  $^1\text{H}$  NMR (400 MHz,  $\text{DMSO}-d_6$ )  $\delta$  7.90 (d,  $J = 7.5$  Hz, 2H), 7.74 (d,  $J = 7.4$  Hz, 2H), 7.48 – 7.28 (m, 4H), 4.34 – 4.17 (m, 3H), 3.87 (qd,  $J = 17.3, 6.1$  Hz, 2H), 3.66 – 3.50 (m, 2H), 2.79 (q,  $J = 14.6$  Hz, 4H), 2.42 – 2.28 (m, 2H), 2.12 – 1.84 (m, 4H).

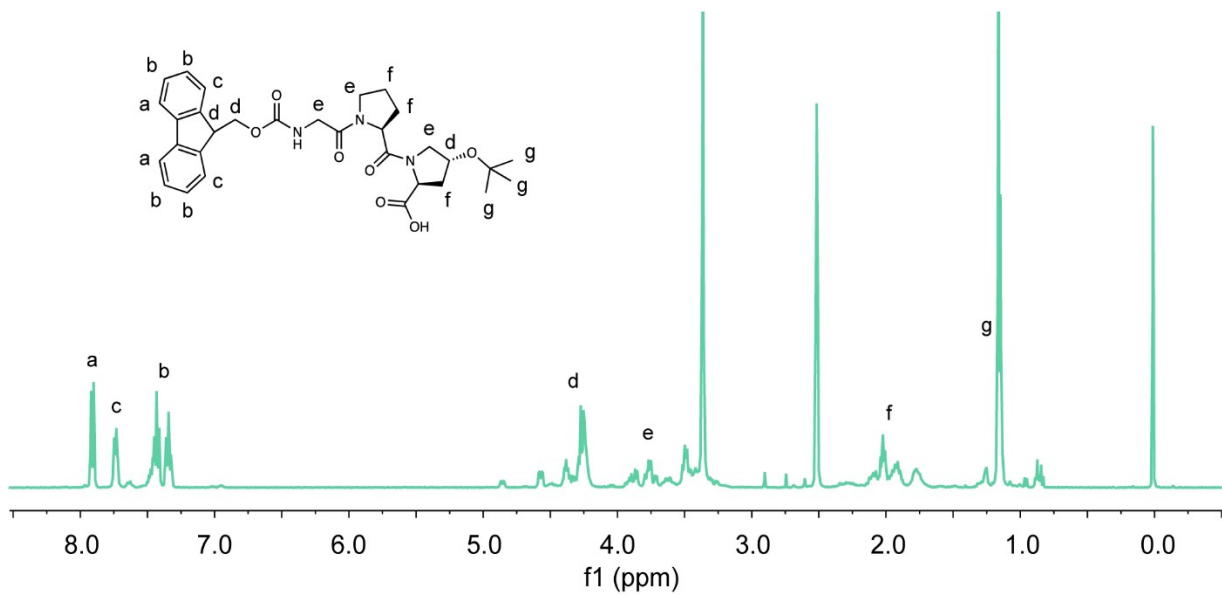


**Figure S15:**  $^1\text{H}$ NMR spectrum of Fmoc-GPO(tBu)-OH.  $^1\text{H}$  NMR (400 MHz,  $\text{DMSO}-d_6$ )  $\delta$  7.90 (d,  $J = 7.5$  Hz, 2H), 7.73 (t,  $J = 6.0$  Hz, 2H), 7.46 – 7.30 (m, 4H), 4.43 – 4.15 (m, 6H), 3.98 – 3.55 (m, 6H), 2.05 – 1.84 (m, 4H), 1.83 – 1.68 (m, 2H), 1.15 (d,  $J = 6.4$  Hz, 9H).

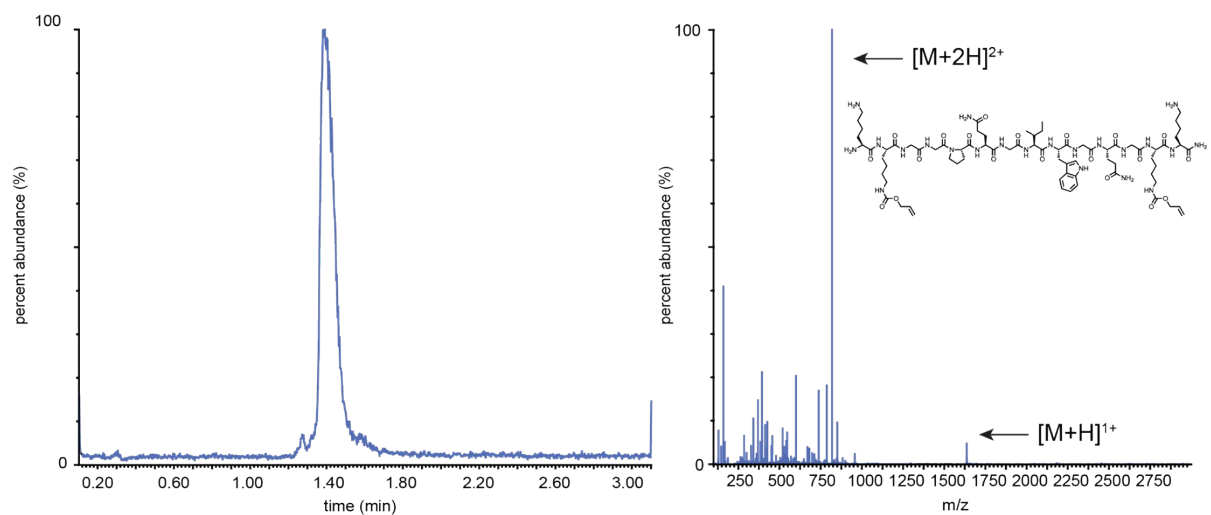


**Figure S16:** UPLC trace and ESI+ spectrum for linker peptide KK(aloc)GGPQGIWGQGK(aloc)K. Single Quadrupole Detector 2 (SQD2) UPLC trace and ESI+ mass spectrometry confirmed the desired product with expected molecular weight of 1635 g/mol ( $[M+H]^+$  = 1636 g/mol and  $[M+2H]^{2+}$  = 818 g/mol).

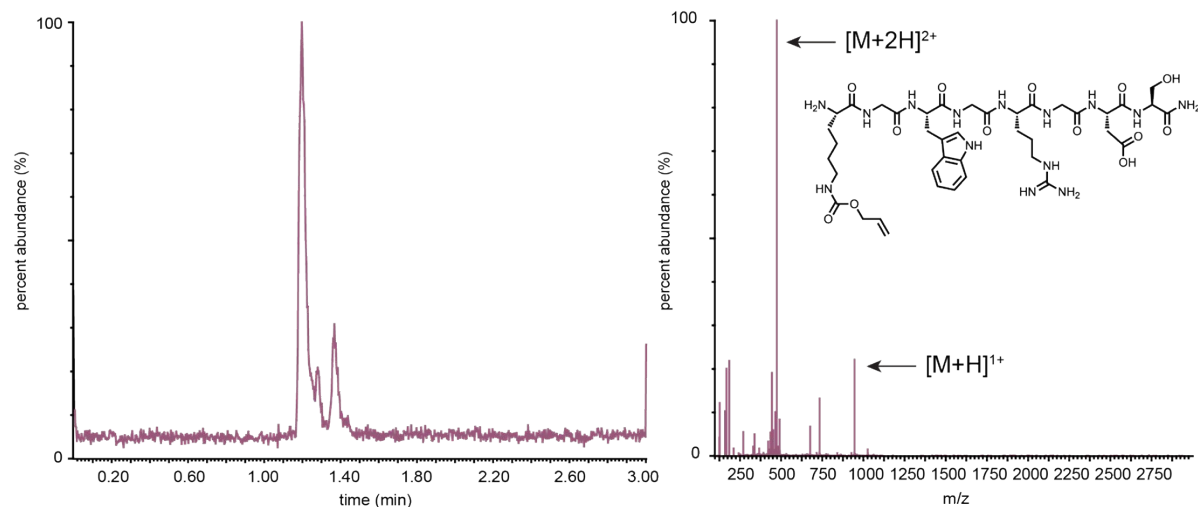


**Figure S17:** UPLC trace and ESI+ spectrum for integrin binding peptide K(aloc)GWGRGDS. Single Quadrupole Detector 2 (SQD2) UPLC trace and ESI+ mass spectrometry confirmed the desired product with expected molecular weight of 945 g/mol ( $[M+H]^{+}$  = 946 g/mol and  $[M+2H]^{2+}$  = 473 g/mol).

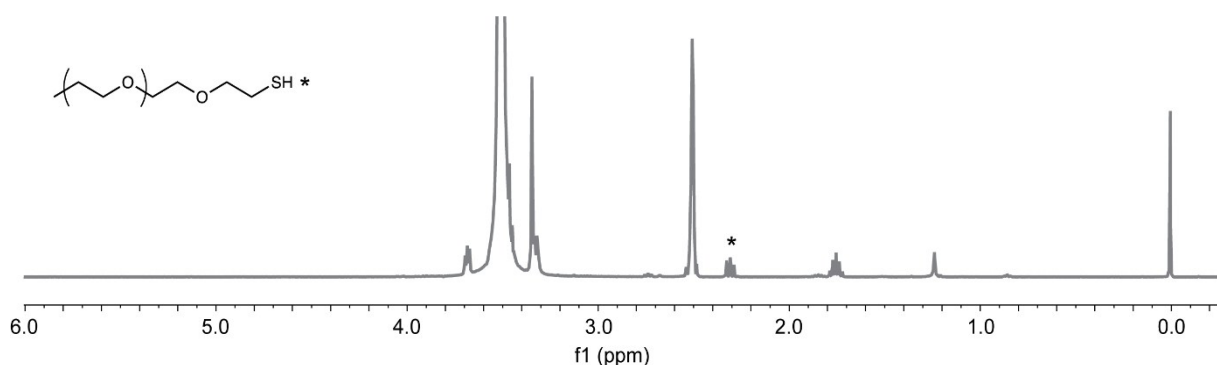


**Figure S18:**  $^1\text{H}$ NMR spectrum of PEG-4-SH.  $^1\text{H}$ NMR (400 MHz,  $\text{DMSO-}d_6$ ):  $\delta$  = 3.69 (s, 454H), 2.51 (d, 13H), 2.36-2.25 (m, 1H), 1.75 (p, 2H). Peak at 3.69 ppm corresponds to the repeat units within the 4-arm PEG backbone and was assigned an integration value of 454H. Integration of the thiol proton (starred peak) was normalized to the integration of the PEG backbone protons to determine functionality (typically  $\sim 95\%$  as shown here).

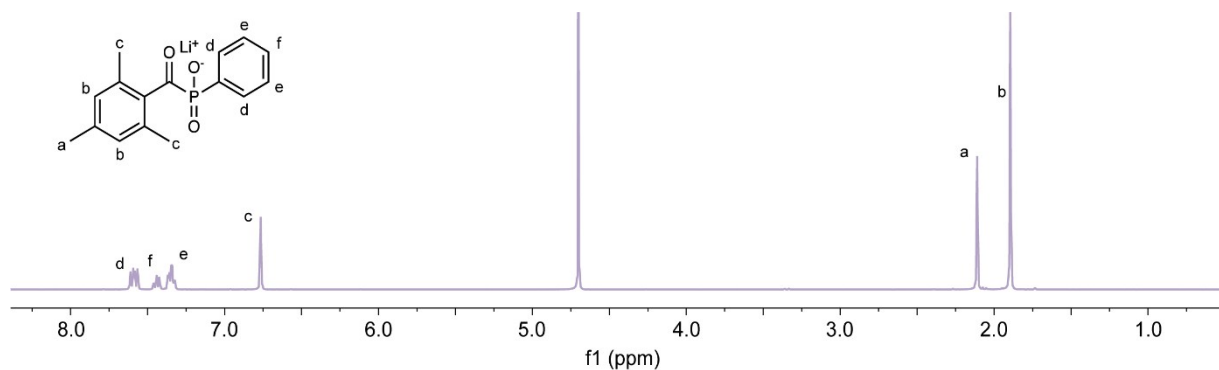


**Figure S19:**  $^1\text{H}$ NMR spectrum of LAP photoinitiator.  $^1\text{H}$  NMR (400 MHz, Deuterium Oxide)  $\delta$  7.63 – 7.54 (m, 2H), 7.48 – 7.41 (m, 1H), 7.34 (tdd,  $J$  = 6.8, 3.1, 1.3 Hz, 2H), 6.77 (s, 2H), 2.11 (s, 3H), 1.89 (s, 6H).

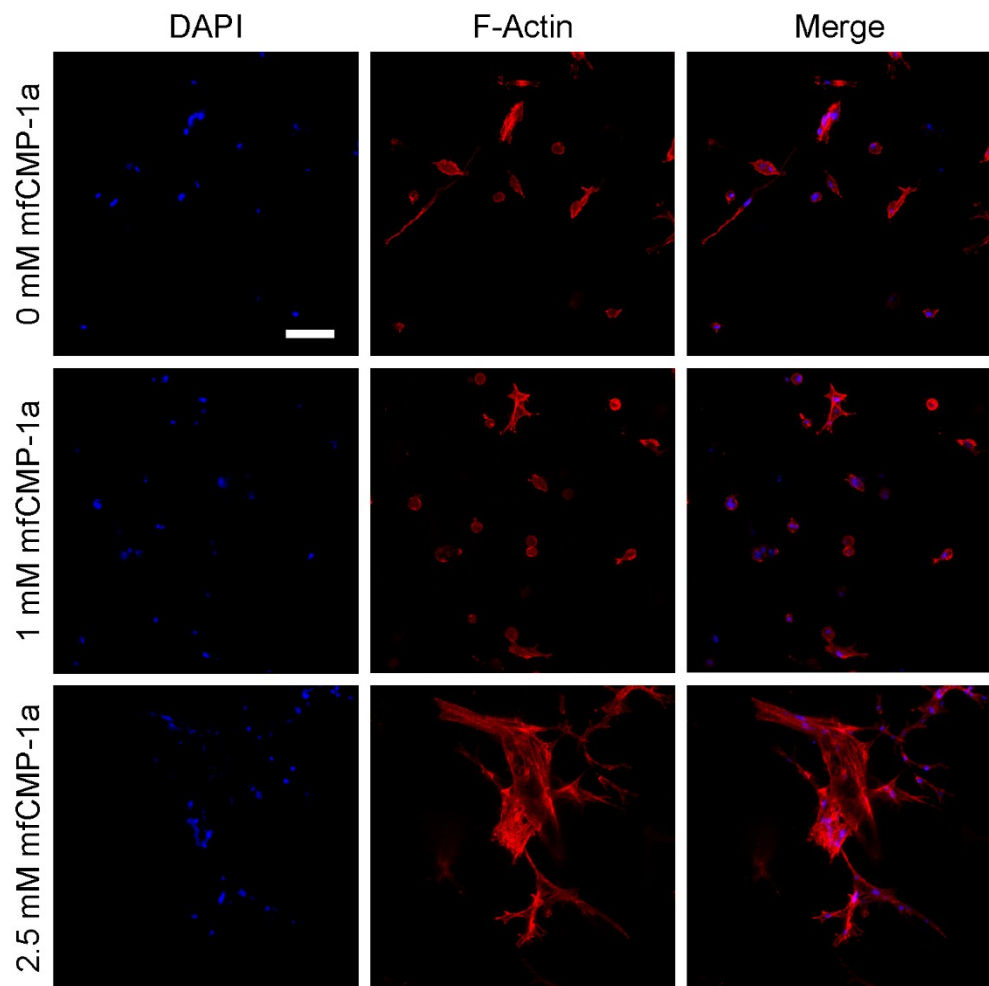


**Figure S20:** Day 10 image splits of cells cultured within hydrogels with mfCMP-1a. Representative maximum intensity projections (from z-stacks, 200  $\mu\text{m}$  thick) of hMSCs encapsulated within hydrogels without mfCMP-1a (0 mM), at a low concentration (1 mM), or at a high concentration (2.5 mM) of mfCMP-1a. Cell nuclei are blue (left, DAPI), cell bodies are red (center, F-Actin), and the merged images are shown on the right. Scale bar = 100  $\mu\text{m}$ .

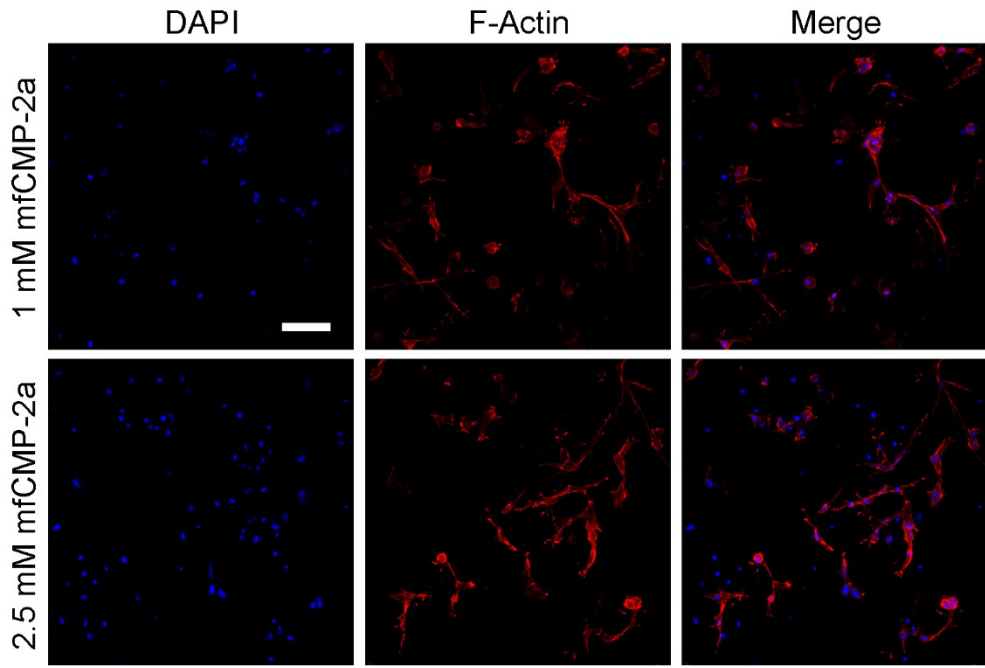


**Figure S21:** Day 10 image splits of cells cultured within hydrogels with mfCMP-2a. Representative maximum intensity projections (from z-stacks, 200  $\mu\text{m}$  thick) of hMSCs encapsulated within hydrogels at a low concentration (1 mM) or at a high concentration (2.5 mM) of mfCMP-2a. Cell nuclei are blue (left, DAPI), cell bodies are red (center, F-Actin), and the merged images are shown on the right. Scale bar = 100  $\mu\text{m}$ .

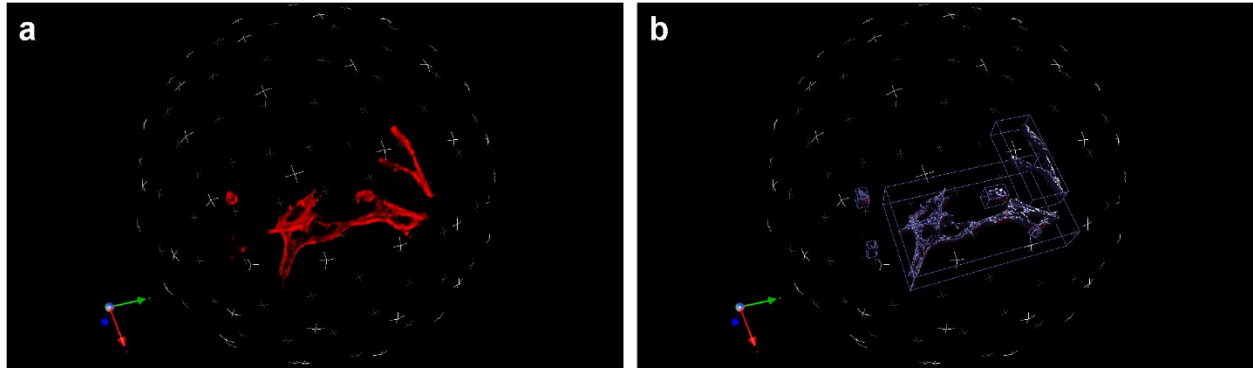


**Figure S22:** Velocity processing for shape factor analysis. **a)** An example 3D rendering of a confocal z-stack (200  $\mu\text{m}$  thick) allows for visualization of cell interactions in the z direction in addition to the traditional x and y directions. **b)** Through Velocity processing (as described in the Methods section) we are able to isolate objects (either single cells or multiple cells in contact) and calculate the object surface area and volume in order to determine the shape factor.

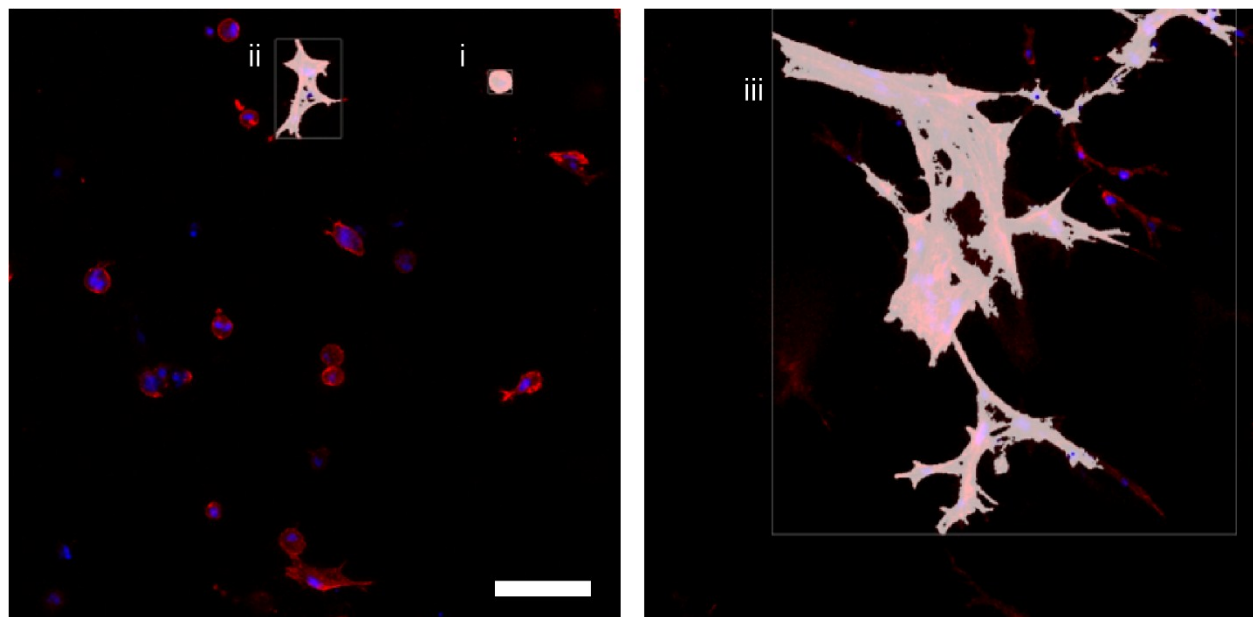


**Figure S23:** Velocity shape factor analysis and binning examples. Example images of cells in hydrogels with 1 mM mfCMP-1a (left) or 2.5 mM mfCMP-1a (right) demonstrating classification of objects (single cells or groups of cells in contact) as *rounded* (i), *spread* (ii), and *elongated* (iii). Scale bar = 100  $\mu$ m.